Plant Biotechnology Journal
Open Access

Plant Biotechnology Journal (2020) **18**, pp. 929–943 doi: 10.1111/pbi.13257

Characterizing the involvement of *FaMADS9* in the regulation of strawberry fruit receptacle development

José G. Vallarino[1,2,†], Catharina Merchante[1,†], José F. Sánchez-Sevilla[2,3], María AngelsdeLuis Balaguer[4,a], Delphine M. Pott[1,2], María T. Ariza[1,2], Ana Casañal[1], David Posé[1,2], Amalia Vioque[1], Iraida Amaya[2,3], Lothar Willmitzer[5], Roberto Solano[6], Rosangela Sozzani[4,7], Alisdair R. Fernie[5], Miguel A. Botella[1,2], James J. Giovannoni[8], Victoriano Valpuesta[1,2]* and Sonia Osorio[1,2]*

[1]*Departamento de Biología Molecular y Bioquímica. Campus de Teatinos, Instituto de Hortofruticultura Subtropical y Mediterránea 'La Mayora', Universidad de Málaga-Consejo Superior de Investigaciones Científicas, Málaga, Spain*

[2]*Unidad Asociada IFAPA-CSIC Biotecnología y Mejora en Fresa, Málaga, Spain*

[3]*Genómica y Biotecnología, Centro de Málaga, Instituto Andaluz de Investigación y Formación Agraria y Pesquera (IFAPA), Málaga, Spain*

[4]*Plant and Microbial Biology Department, North Carolina State University, Raleigh, NC, USA*

[5]*Max-Planck-Institut für Molekulare Pflanzenphysiologie, Potsdam-Golm, Germany*

[6]*Departmento de Genética Molecular de Plantas, Centro Nacional de Biotecnología, Consejo Superior de Investigaciones Científicas (CNB-CSIC), Madrid, Spain*

[7]*Biomathematics Program, North Carolina State University, Raleigh, NC, USA*

[8]*Boyce Thompson Institute for Plant Research and USDA-ARS, Robert W. Holley Center, Cornell University Campus, Ithaca, NY, USA*

Received 5 November 2018;
revised 3 September 2019;
accepted 8 September 2019.
**Correspondence* (Tel +34 952131932; email valpuesta@uma.es (V.V.) and Tel +34 952134271; email sosorio@uma.es (S.O.))
Present address: Precision Biosciences, Inc., Durham, NC, USA
[†]These authors contributed equally to the article.

Keywords: strawberry, fruit ripening, quality.

Abstract

FaMADS9 is the strawberry (*Fragaria x ananassa*) gene that exhibits the highest homology to the tomato (*Solanum lycopersicum*) *RIN* gene. Transgenic lines were obtained in which *FaMADS9* was silenced. The fruits of these lines did not show differences in basic parameters, such as fruit firmness or colour, but exhibited lower Brix values in three of the four independent lines. The gene ontology MapMan category that was most enriched among the differentially expressed genes in the receptacles at the white stage corresponded to the regulation of transcription, including a high percentage of transcription factors and regulatory proteins associated with auxin action. In contrast, the most enriched categories at the red stage were transport, lipid metabolism and cell wall. Metabolomic analysis of the receptacles of the transformed fruits identified significant changes in the content of maltose, galactonic acid-1,4-lactone, proanthocyanidins and flavonols at the green/white stage, while isomaltose, anthocyanins and cuticular wax metabolism were the most affected at the red stage. Among the regulatory genes that were differentially expressed in the transgenic receptacles were several genes previously linked to flavonoid metabolism, such as *MYB10*, *DIV*, *ZFN1*, *ZFN2*, *GT2*, and *GT5*, or associated with the action of hormones, such as abscisic acid, *SHP*, *ASR*, *GTE7* and *SnRK2.7*. The inference of a gene regulatory network, based on a dynamic Bayesian approach, among the genes differentially expressed in the transgenic receptacles at the white and red stages, identified the genes *KAN1*, *DIV*, *ZFN2* and *GTE7* as putative targets of *FaMADS9*. A *MADS9*-specific CArG box was identified in the promoters of these genes.

Introduction

Strawberry is a non-climacteric fruit, and several studies have analysed the metabolic (Fait *et al.*, 2008) and cell wall changes (Jiménez-Bermúdez *et al.*, 2002; Quesada *et al.*, 2009) that occur during fruit ripening, as well as changes in gene expression associated with this process (Aharoni and O'Connell, 2002; Härtl *et al.*, 2017; Pillet *et al.*, 2015; Sánchez-Sevilla *et al.*, 2017). Recently, a number of reports have shed light on two key elements of the strawberry fruit developmental programme of strawberry fruit: the involvement of hormones and the participation of specific transcription factors.

Early studies reported that auxin plays an essential role in the regulation of strawberry fruit growth and ripening because the growth of the green receptacles is dependent on auxin delivery from the achenes (Mezzetti *et al.*, 2004; Nitsch, 1950). However, a recent analysis of the transcriptome in developing fruits showed significant expression of several auxin biosynthetic and signalling genes in the ripening receptacles (Estrada-Johnson *et al.*, 2017). In addition to auxin, other hormones have been reported to be involved in fruit development, such as gibberellins (Csukasi *et al.*, 2011), abscisic acid (Chai *et al.*, 2011; Jia *et al.*, 2011), jasmonates (Concha *et al.*, 2013; Mukkun and Singh, 2009) and brassinosteroids (Chai *et al.*, 2013). In contrast to the situation in climacteric fruits, ethylene does not play a key role in the onset of the ripening process (Perkins-Veazie, 1995). However, Merchante *et al.* (2013) described a role for this hormone in some specific ripening-associated molecular changes, despite the lack of a general effect on fruit ripening.

Studies regarding the regulatory genes of the strawberry fruit ripening process are limited, and most of the studies have examined the roles of these genes in the metabolic changes that occur with ripening. In this context, two transcription factors (TFs), namely *FaMYB1* and *FaMYB10*, have been reported to play a major role in the regulation of

phenylpropanoid, flavonoid and anthocyanin biosynthesis during ripening (Aharoni *et al.*, 2001; Lin-Wang *et al.*, 2010; Medina-Puche *et al.*, 2014). Additionally, studies on the three components of the complex that regulates flavonoid synthesis identified four TFs, namely FaMYB9/FaMYB11, FabHLH3 and FaTTG1, as positive regulators of the biosynthesis of proanthocyanidins (Schaart *et al.*, 2013). Correlation analysis of the transcriptomes of ripening fruits also identified three TFs of the MYB, TCP and SCL families that were positively correlated with flavonoid accumulation in ripening fruits (Pillet *et al.*, 2015). Recently, other TFs have been reported to regulate the gene expression of eugenol synthase2 (Medina-Puche *et al.*, 2015; Molina-Hidalgo *et al.*, 2017), which is involved in the synthesis of eugenol (Aragüez *et al.*, 2013).

To date, few TFs have been identified as being linked to the role of hormones in strawberry fruit ripening. That said, we previously identified a *GAMYB* TF gene, *FaGAMYB*, as a key regulatory player in the initiation of strawberry receptacle ripening that acts upstream of ABA and sucrose signalling (Vallarino *et al.*, 2015). It has also been proposed that the C-type MADS-box gene SHATTERPROOF-like (*FaSHP)* might play a modulatory role in strawberry fruit ripening acting, either directly or indirectly, via other TFs during the transition from auxin-to ABA-mediated control (Daminato *et al.*, 2013).

In climacteric fruit such as tomato, the RIN transcription factor has been linked to ripening-associated enhancement of ethylene levels (Giovannoni, 2007; Vrebalov *et al.*, 2002). Recently, by examination of *RIN* knockout mutants, RIN was shown to be required for complete normal ripening of tomato fruits (Ito *et al.*, 2017). Similarly, homologous MADS-box genes in other species have been reported to play a major role in the development and ripening of other climacteric fruits, such as peach (Tadiello *et al.*, 2009), banana (Elitzur *et al.*, 2010) and oil palm (Tranbarger *et al.*, 2011). In non-climacteric fruits such as bilberry (Jaakola *et al.*, 2010), the putative orthologue of the tomato *RIN* has been demonstrated to be involved in fruit ripening. In strawberry, silencing of the *FaMADS9* gene, an orthologue of the tomato *RIN*, altered the normal development of the achene and receptacle, and transcriptomic analysis of the silenced fruits revealed pleiotropic effects on gene expression (Seymour *et al.*, 2011). By analysis of the strawberry fruit transcriptome, we found that *FaMADS9* presented weak expression in the achenes and high expression in the receptacles, showing two main peaks, one at the green developmental stage and the other at the red developmental stage (Sánchez-Sevilla *et al.*, 2017). In this work, we complement the preliminary study of this gene (Seymour *et al.*, 2011) via the generation of four independent strawberry transgenic lines that were silenced in the *FaMADS9* gene and present an in-depth analysis. Our data support a major role of the *FaMADS9* gene in not only the orchestration of the metabolic changes that occur during fruit ripening, but also the possible involvement of auxin and abscisic acid in the fruit developmental programme, and, in particular, in the formation and synthesis of the fruit cuticle.

Results

Silencing of *FaMADS9* does not produce a visually apparent phenotype in strawberry fruits

To dissect the role played by *FaMADS9* in the ripening receptacles, we performed stable RNAi-mediated *FaMADS9* gene silencing in plants of the Camarosa cultivar. Four transgenic lines (L6, L7, L23 and L27) were selected based on the significant reduction in *FaMADS9* expression in these lines. Although phenotypic differences between control and *FaMADS9*-silenced lines were reported when the cultivar Calypso was used (Seymour *et al.*, 2011), the transformed fruits herein showed a normal appearance (Figure 1a). Analysis of other fruit characteristics, such as firmness and total soluble solid content (Brix), showed that three of the silenced lines (L7, L23 and L27) exhibited a significantly reduced Brix content, whereas no significant changes were observed in fruit firmness (Figure 1b,c). Given that *FaMADS9* is expressed in the early stage of achene development (Sánchez-Sevilla *et al.*, 2017), as well as in flowers (Seymour *et al.*, 2011), we next evaluated the effect of *FaMADS9* silencing on fruit abortion and fruit yield. The silenced lines exhibited no significant changes in these traits (Figure 1d,e).

Evaluation of the changes in the receptacle transcriptome of silenced lines identifies regulatory genes associated with hormone activity

The two silenced lines (L6 and L7) that showed strong reduction in *FaMADS9* expression and the control were selected for RNA sequencing (RNAseq) expression analysis of the receptacles at two different stages, white and red (Figure 1f,g; Table S1). Because the reads were mapped on the *Fragaria vesca* genome (Edger *et al.*, 2018), the differentially expressed genes were named hereafter based on the orthologue in *F. vesca*. At the white stage, a total of 2670 genes were significantly differentially expressed, while at the red stage, 1943 genes were differentially expressed (Table S2). Notably, only one of the 34 *MADS* genes expressed in fruits (Sánchez-Sevilla *et al.*, 2017) was down-regulated in the silenced receptacles, namely *FaMADS9* (*FvH4_6g46420*), the expression of which decreased more than 90% in both the white and red stages (Figure 1f). This result was confirmed when the expression was evaluated by qRT-PCR (Figure 1g). However, another *FaMADS* gene, namely *SHATTERPROOF1-like* (*SHP1*; *FvH4_6g37880*), was up-regulated in both the white and red receptacles (Table S3; Figure S1). The differential expression of these two *MADS* genes was also confirmed by qRT-PCR, as was the expression of three other *MADS* genes (*FvH4_3g06720*, *FvH4_5g13510* and *FvH4_5g35410*) that were not differentially expressed in the RNAseq study (Table S3, Figure S1).

Analysis of the enriched functional MapMan categories (Thimm *et al.*, 2004) of the differentially expressed genes was performed at the two developmental stages (Table S4). In the white receptacle, the most enriched category corresponded to RNA (Bincode '27.3'; 26%) (Figure 2a), which included many TFs (over 82%). Among the TF families, the sub-category of auxin response factors (*ARFs)* (Bincode '27.3.4') was also enriched. This category included nine members of the *ARF* family from the seventeen that are expressed in strawberry fruits (Estrada-Johnson *et al.*, 2017), all but one (*ARF16c*) of which were down-regulated, mostly at the white stage (Table S5). Additionally, there was a change in the expression of seven members of the regulatory *AUX/IAA* genes, all of which were down-regulated by *IAA11* (Table S5). The only two genes associated with auxin metabolism that were differentially expressed in the transgenic receptacles were *GH3.6* (*FvH4_2g24250*), which was up-regulated in the white receptacles, and *GH3.17* (*FvH4_ 4g22430*), which was down-regulated in red receptacles (Table S5). The next most enriched subcategory was the DOF family of TFs (Bincode '27.3.8'), which included *FaDOF1* (*FvH4_5g05330*) and *FaDOF2* (*FvH4_2g14390*),

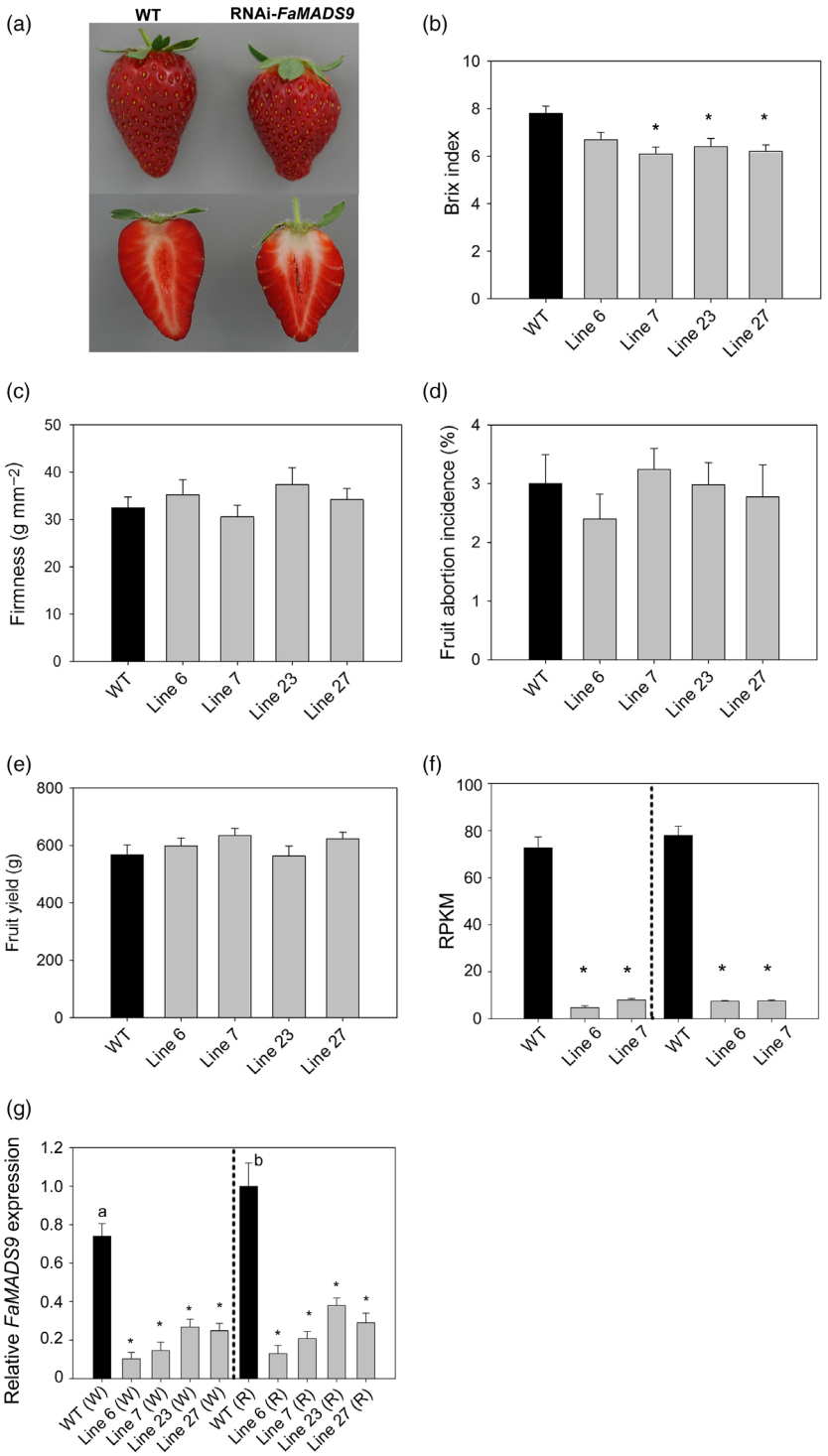

Figure 1 Preliminary characterization of *FaMADS9*-silenced lines. (a) Photographs of the ripe fruits of the WT and *FaMADS9*-silenced line. (b) Total soluble solid content (Brix index). (c) Firmness analysis. (d) Fruit abortion incidence. (e) Total fruit yield. (f) Expression of the *FaMADS9* gene in L6 and L7 in the receptacle and two developmental stages (white and red) by RNAseq. FPKM, fragments per kilobase of exon per million fragments mapped. (g) Expression of *FaMADS9* gene in white and ripe fruits of the transgenic lines (L6, L7, L23 and L15) and WT. For all parameters, values are presented as means ± SE of nine biological replicates (for RNAseq analysis, three biological replicates were used). Different letters indicate a significant difference between samples according to the corresponding ANOVA ($P < 0.05$). Asterisks indicate values that were determined by Student's *t*-test to be significantly different ($P < 0.05$) from the wild type (WT).

the latter being involved in eugenol production in the ripe receptacles (Molina-Hidalgo *et al.*, 2017). While *FaDOF1* was down-regulated in the white receptacles of the transgenic lines, *FaDOF2* was up-regulated (Table S2).

Cell growth processes and energetic metabolism were altered in the silenced lines

The next most enriched MapMan category in the white receptacles was miscellaneous (Bincode '26'; 20%) (Figure 2a), which includes a diverse group of genes, prominent among which are the UDP-glucosyl/glucuronosyl transferases (32 genes) (Table S4). The enrichment of this MapMan category, along with other highly represented categories such as cell (Bincode '31'; 12%), cell wall (Bincode '10'; 10%) and transport (Bincode '34'; 15%) (Figure 2a; Table S4), suggests a considerable role of *FaMADS9* in the growth processes associated with early-stage receptacle development. Thus, the third most enriched category, transport, included 12 genes corresponding to major intrinsic proteins (NIP,

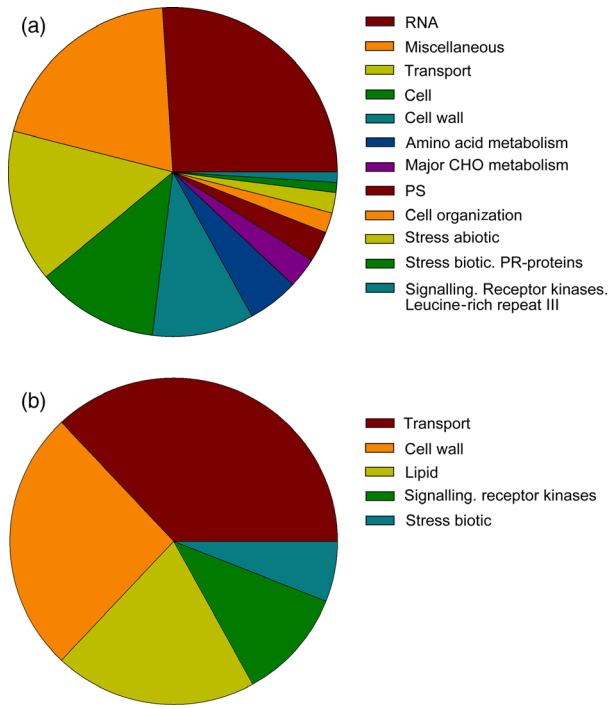

Figure 2 Enriched categories of genes differentially expressed in *FaMADS9*-silenced receptacle. Functional distribution is given for those genes showing significant ($P < 0.05$) differential expression values in transgenic fruits, based on MapMan classification at white (a) and red (b) stages.

PIP and TIP), 9 of which were down-regulated in the transgenic lines (Table S6). One annotated as *NIP1-1*-like aquaporin *(FvH4_6g08000)* was up-regulated in the white receptacles.

Metabolic changes in the receptacles of *FaMADS9*-silenced lines lead to alterations in starch and ascorbate metabolism

Various metabolic categories were enriched in the differentially expressed genes: carbohydrates and amino acids in the white receptacles (Figure 2a) and lipids in the red receptacles (Figure 2b). Therefore, primary metabolites were analysed in the receptacles of the four silenced lines (L6, L7, L23 and L27) at the green, white and red stages. Both principal component analysis (Figure S2a) and hierarchical clustering analysis (Figure S2b) clearly grouped the samples on the basis of developmental stage and genotype. Lines L6 and L7 grouped together at the green and red stages (Figure S2b).

However, the exact pattern of clustering varied among the three stages. A heat map exhibiting the values obtained for all the samples is presented in Figure 3 (Table S7). Metabolic changes were restricted to a few metabolites and only to green and red receptacles. Two of these metabolites are maltose and isomaltose, which are disaccharides produced by the hydrolysis of starch by amylase and isoamylase, respectively. While maltose levels decreased in the green receptacles of the transgenic lines compared to the control, isomaltose levels increased in the red receptacles. These results are consistent with the expression of the strawberry amylase and isoamylase genes in ripening receptacles and their altered expression of these genes in *FaMADS9*-silenced lines. In the white receptacles, the expression of three *ß-amylases* (*FvH4_4g17180*, *FvH4_5g20800* and *FvH4_4g05230*) was significantly decreased in transgenic receptacles, whereas the expression of one *isoamylase* (*FvH4_5g36440*) was enhanced (Table S8). At the red stage, no significant decrease was observed in the *isoamylase levels*, while one *ß-amylase* (*FvH4_4g05230*) was down-regulated and another *ß-amylase* (*FvH4_3g29220*), with very low expression levels, was up-regulated (Table S8).

Another change observed in all the transgenic lines corresponded to galactonic acid-1,4-lactone, the level of which decreased in the receptacles of the transgenic lines, at the white and red stages, compared to the control (Figure 3). Two pathways have been proposed to be responsible for L-ascorbic acid biosynthesis in strawberry, with galactonic acid-1,4-lactone being the final intermediate (Valpuesta and Botella, 2004). Our RNAseq analysis of the silenced receptacles revealed that at the white stage, two genes encoding enzymes of the L-galactose pathway were down-regulated (Table S9). In addition, metabolomic profiling of the green receptacles showed a decrease in ascorbate content in the transgenic lines compared to the control (1.0 ± 0.2; 0.7 ± 0.1; 0.5 ± 0.2; 0.8 ± 0.1; 0.6 ± 0.1 for WT, L6, L7, L23 and L27, respectively; data are normalized to the mean response calculated for the WT). Thus, a diminished flux through the L-ascorbic acid biosynthetic pathway was expected in the transgenic white and red receptacles, which would explain the low galactonic acid-1,4-lactone content at these stages.

The transcriptome of the red receptacles of *FaMADS9*-silenced lines indicates specific changes in the cell wall

Functional analysis of differentially expressed genes in the red receptacles (Table S2) was performed according to the MapMan categories (Thimm *et al.*, 2004). Enriched categories were restricted to four (Figure 2b, Table S4). The most enriched category at this time point was transport (37%). Genes included in this category represent a wide number of gene families associated with very diverse transport systems, with the major intrinsic protein category being highly represented. Five of the twelve genes in this category were down-regulated (Table S6). The next most enriched category was cell wall (Bincode '10'; 26%) (Figure 2b), including an enriched sub-category of cell wall precursor synthesis (Bincode '10.1') (Table S4). Most of the genes down-regulated in this category correspond to the synthesis and modification of cell wall components, such as different classes of proteins and glycopolymers (Table S1).

Since we did not observed differences in the firmness of transgenic fruits (Figure 1c), the expression of genes reported to be involved in cell wall disassembly and degradation during strawberry fruit ripening (Benítez-Burraco *et al.*, 2003; Jiménez-Bermúdez *et al.*, 2002; Molina-Hidalgo *et al.*, 2013; Quesada *et al.*, 2009) was analysed (Table S10). Only polygalacturonases were up-regulated in the transgenic fruits, with both *PG1* (*FvH4_6g41380*) and *PG2* (*FvH4_7g15040*) up-regulated in the white receptacles, and only *PG1* up-regulated in the red receptacles.

Lipid metabolism of epidermal cells of the red receptacles is altered in silenced lines

Lipid metabolism (Bincode '11') is another enriched category (20%) of differentially expressed genes in the ripe receptacle (Figure 2b). In this category, all the genes corresponding to fatty

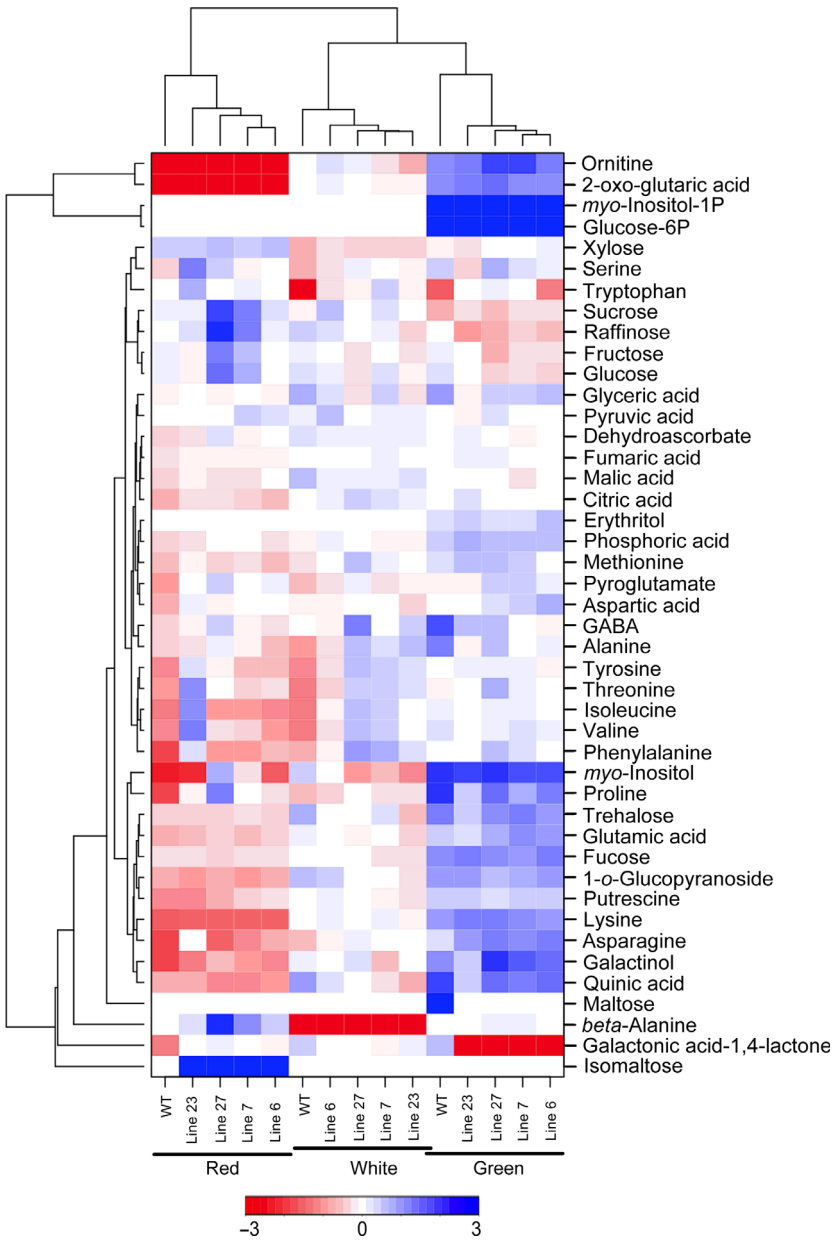

Figure 3 Heat map of primary metabolism in the receptacle of *FaMADS9*-silenced lines at three ripening stages. A colour-coded matrix represents the mean values of the metabolite intensity which has been $\log_2$-transformed and mean-centred.

acid synthesis and elongation were down-regulated, whereas most of the lipases were up-regulated (Tables S1 and S4). In relation to the genes responsible for wax metabolism, several of the putative orthologues of the Arabidopsis genes (Bernard and Joubès, 2013) were down-regulated, at the white and red stages, in particular *CER26* (*FvH4_4g13360*), *CER5/CER7/ABCG12* (*FvH4_3g28460*), *CER6* (*FvH4_4g27420*), *KCR1* (*FvH4_4g25050*), *LACS2* (*FvH4_2g07450*), *HDG1* (*FvH4_7g13350*) and *ß-amyrin 28-oxidase (FvH4_3g11590)* (Table S11). Moreover, the putative orthologue of the *HDG1* gene (*FvH4_7g13350*) in strawberry, a transcriptional regulator of cuticular wax biosynthesis in Arabidopsis (Lee and Suh, 2015), was down-regulated in the white and red receptacles of the silenced lines (Table S11). Other regulatory genes of wax biosynthesis and cuticle formation, such as *WIN1/SHINE1* (*FvH4_6g29930*) and *SHINE3* (*FvH4_2g29150*) (Aharoni *et al.*, 2004; Shi *et al.*, 2013), were also down-regulated in the white receptacles (Table S11). Therefore, we next measured the cuticular wax in ripe fruits of the four *FaMADS9*-silenced lines and the control. There was a significant increase in the content of the highly abundant *n*-alkanes, such as C27- and C29-alkanes, in the four lines, and of C23-alkanes in three of the four lines (Table 1). In addition, the α- and ʌ-amyrin triterpenoid content of the cuticular wax was also significantly enhanced in the four transgenic lines (Table 1). The annotated genes associated with amyrin metabolism that were altered in the transgenic lines were *ß-amyrin 28-oxidase* (*FvH4_3g11590*), which was up-regulated in the white and red receptacles of these lines in comparison with the control and a predicted *ß-amyrin synthase* (*FvH4_6g36520*), which was also up-regulated, but only in the white receptacles (Table S11); the latter is the first enzyme proposed to modify *ß*-amyrin into oleanolic acid (Han *et al.*, 2013).

Waxes cover or are embedded into the cutin polymer, forming the plant cuticle (Domínguez *et al.*, 2015). Since we found

changes in the epicuticular wax, we focused on the other component of the cuticle, the cutin. For this purpose, we evaluated the expression of the strawberry orthologue (*FvH4_6g01380*) of the cutin synthases of tomato, *CD1* (Yeats *et al.*, 2012a); the orthologue was down-regulated in the transgenic lines at the white stage (Table S11). The differential expression of this gene along with two selected wax biosynthesis genes, namely *CER2* and *CER26*, was checked by qPCR in the white and red receptacles (Figure S3a). Silencing of *CER26* and *CD1* was confirmed, while silencing of *CER2* was significant only at the white stage. Analysis of the expression of these genes in different fruit parts shows that *CER26* and *CD1* are mostly expressed in the epidermal cell-enriched surface of the fruit (Figure S3b).

In tomato fruits, it has been reported that cuticular wax composition is changed in ABA-deficient mutants (Martin *et al.*, 2017). Previous studies have shown that ABA plays an important role in the regulation of strawberry fruit ripening (Chai *et al.*, 2011; Jia *et al.*, 2011; Li *et al.*, 2015). Here, we found that three key genes involved in the synthesis of ABA, namely *NCED1* (*FvH4_3g16740*), *NCED2* (*FvH4_3g05440*) and *NCED3* (*FvH4_3g16730*), the expression of which increases during receptacle ripening (Sánchez-Sevilla *et al.*, 2017), were significantly down-regulated (over 70%) in the red receptacles of *FaMADS9*-silenced lines (Table S2). Then, the ABA level was measured in the receptacles of the transgenic fruits and the control. The results showed a reduction in all the lines between 22% and 49% (Table S12).

Secondary metabolism in the red receptacle of silenced lines shows clear changes in the phenylpropanoid pathway

Although there was not an apparent colour change phenotype in the fruits of the transgenic lines (Figure 1a), due to the elevated number of DE genes in transgenic receptacles (Table S2), changes in other colourless secondary metabolites were expected. Thus, analysis of secondary metabolism was performed in the receptacle of four independent transgenic lines at the green, white and red stages (Figure 4; Table S13). At the green stage, there was an increase in procyanidins, propelargonidins and flavan-3-ols levels in the transgenic lines. In contrast, the levels of galloyl derivatives, quercetin and kaempferol derivatives, terpenoid derivatives, eriodictyol hexoses, and ellagitannins were diminished in the green receptacles of the transgenic lines. In the case of ellagitannins, two glycosyltransferases (GTs) that are involved in ellagitannin metabolism (*FvH4_2g05060* and *FvH4_2g05090*) (Schulenburg *et al.*, 2016) were up-regulated in the transgenic green receptacles (Table S2). Significant changes in the red receptacles were observed in the levels of naringenin chalcone hexose, which increased, and the anthocyanins (Figure 4; Table S13). Of the anthocyanins, while the cyanidin derivative content was low in the transgenic receptacles, the pelargonidin derivative content was high. Other compounds, such as ellagic acid, its derivatives, and hydroxycinnamic acid and benzoic acid derivatives, were invariant across the genotypes at all the developmental stages studied.

Table 1 Wax constituents in *FaMADS9*-silenced fruits (relative per cent) identified in strawberry cuticles at the red stage.

Wax constituents	WT	L6	L7	L23	L27
n-alkanes					
Docosane (C22)	0.1 ± 0.0	0.1 ± 0.0	0.1 ± 0.1	0.1 ± 0.0	0.1 ± 0.1
Tricosane (C23)	2.1 ± 0.3	2.6 ± 0.4	**4.1 ± 0.5**	**4.9 ± 0.3**	**5.8 ± 0.4**
Tetracosane (C24)	0.2 ± 0.1	0.1 ± 0.1	0.2 ± 0.1	0.2 ± 0.1	0.1 ± 0.1
Hexacosane(C26)	0.3 ± 0.1	0.3 ± 0.2	0.3 ± 0.1	0.2 ± 0.1	0.3 ± 0.1
Heptacosane (C27)	3.7 ± 0.2	**5.2 ± 0.3**	**6.9 ± 0.3**	**7.3 ± 0.6**	**6.5 ± 0.4**
Octacosane (C28)	0.4 ± 0.1	0.3 ± 0.1	0.4 ± 0.0	0.3 ± 0.1	0.4 ± 0.1
Nonacosane (C29)	7.1 ± 0.7	**13.8 ± 0.3**	**15.9 ± 0.5**	**14.4 ± 0.8**	**18.6 ± 0.9**
Triacontane (C30)	0.8 ± 0.2	0.7 ± 0.2	1.0 ± 0.3	1.1 ± 0.3	0.9 ± 0.3
Hentriacontane (C31)	0.1 ± 0.0	0.2 ± 0.1	0.1 ± 0.1	0.2 ± 0.2	0.1 ± 0.1
Dotriacontane (C32)	0.6 ± 0.1	0.5 ± 0.2	0.5 ± 0.2	0.6 ± 0.3	0.7 ± 0.2
iso-alkanes					
2-methyl triacontanol (iso-C31)	2.4 ± 0.5	2.9 ± 0.7	2.2 ± 0.6	2.7 ± 0.6	2.2 ± 0.8
2-methylhentriacontane (iso-C32)	0.3 ± 0.1	0.2 ± 0.1	0.3 ± 0.1	0.2 ± 0.2	0.3 ± 0.1
n-alkan-1-ols					
Docosanol (C22)	1.4 ± 0.5	1.1 ± 0.4	1.7 ± 0.5	1.1 ± 0.5	1.5 ± 0.3
Tricosanol (C23)	2.2 ± 0.5	2.0 ± 0.3	1.9 ± 0.4	2.2 ± 0.5	1.9 ± 0.5
Tetracosanol (C24)	0.2 ± 0.1	0.2 ± 0.0	0.2 ± 0.2	0.2 ± 0.1	0.1 ± 0.1
Hexacosanol (C26)	0.3 ± 0.1	0.3 ± 0.1	0.3 ± 0.2	0.2 ± 0.2	0.3 ± 0.1
Octacosanol (C28)	0.5 ± 0.1	0.5 ± 0.3	**0.7 ± 0.1**	**0.7 ± 0.1**	**0.9 ± 0.2**
Nonacosanol (C29)	0.2 ± 0.1	0.1 ± 0.1	0.2 ± 0.1	0.2 ± 0.2	0.2 ± 0.1
Triacontanol (C30)	0.3 ± 0.1	0.2 ± 0.2	0.3 ± 0.1	0.4 ± 0.1	0.3 ± 0.1
Amyrins					
α	4.7 ± 0.6	**16.3 ± 0.5**	**11.6 ± 0.4**	**15.8 ± 0.5**	**18.3 ± 0.6**
ß	8.9 ± 0.5	9.4 ± 0.6	7.8 ± 0.6	8.6 ± 0.7	9.9 ± 0.7
Δ	17.7 ± 0.4	**20.5 ± 0.5**	**22.8 ± 0.4**	**19.9 ± 0.2**	**24.3 ± 0.6**

Data in bold indicate statistically significant differences from WT as determined by Student's *t*-test ($P < 0.05$).

These changes in secondary metabolites along with changes in the expression of genes involved in their associated biosynthetic pathways are summarized in Figure 5. In addition to the diminished expression of the *4-coumarate-coenzyme ligase (4CL)* genes in the white receptacles (Table S14), there was an increase in the expression of genes involved in the first steps of the flavonoid pathway (*CHS1*, *FvH4_7g01160*; *CHI1*, *FvH4_7g20870*; *CHI3*, *FvH4_7g25890*; *F3H*, *FvH4_1g11810*) (Table S1), which may explain the increase in proanthocyanidins levels in the green receptacles (Figures 4 and 5). The down-regulation of the *FLS3* gene (*FvH4_5g29430*) in the silenced receptacles would explain the decreased levels of flavonols and their derivatives that were observed in the green receptacles (Figures 4 and 5). At the red stage, the only significant changes in gene expression corresponded to the early genes of the phenylpropanoid pathway, such as *PAL1* (*FvH4_6g16060*), *PAL2 (FvH4_7g19130)*, *C4H (FvH4_3g40570)*, *4CL* (Table S14), and *F3H* (*FvH4_1g11810*) which were down-regulated (Figure 5). This diminution was enhanced for the *PAL* genes and should affect all of the downstream metabolites in the pathway. The down-regulation of *F3′H* (*FvH4_5g14010*) at the white stage (Figure 5; Table S1) would explain the diminished content of cyanidin hexose in the red receptacles of transgenic fruits (Figure 4; Table S13).

The analysis of *MYB10* (*FvH4_1g22020*), a gene involved in the regulation of the flavonoid pathway in strawberry fruits (Medina-Puche *et al.*, 2014), showed that the expression of this gene was significantly up-regulated in the white receptacles (Table S2). Other TFs for which expression was correlated with flavonoid metabolism, such as *TCP1* (*FvH4_6g16170*), *ZFN2 (FvH4_7g01060)* and *DIV (FvH4_6g11950)* (Pillet *et al.*, 2015), were down-regulated in transgenic red receptacles (Table S2). In contrast, other genes associated with anthocyanin production in strawberry, such as the four members of the *RAP* family (*FvH4_1g27460*, *FvH4_6g38760*, *FvH4_2g25200*, *FvH4_2g25210*), encoding GST anthocyanin transporters (Luo *et al.*, 2018), were up-regulated in white receptacles of the silenced lines.

Analysis of the gene regulatory network in the ripening receptacles identified transcription factors associated with *FaMADS9*

The high number of differentially expressed genes found in the *FaMADS9*-silenced fruits reveals the key role played by the *FaMADS9* gene in the fruit ripening process and is a consequence of both direct and indirect transcriptional effects of the gene silencing. To gain insight into the possible relationships among these differentially expressed genes, two gene expression data sets were used to infer a gene regulatory network (GRN). GRN inference was performed using GENIST, based on a dynamic Bayesian network (DBN) inference algorithm, which has exceptional utility when starting from time course or developmental

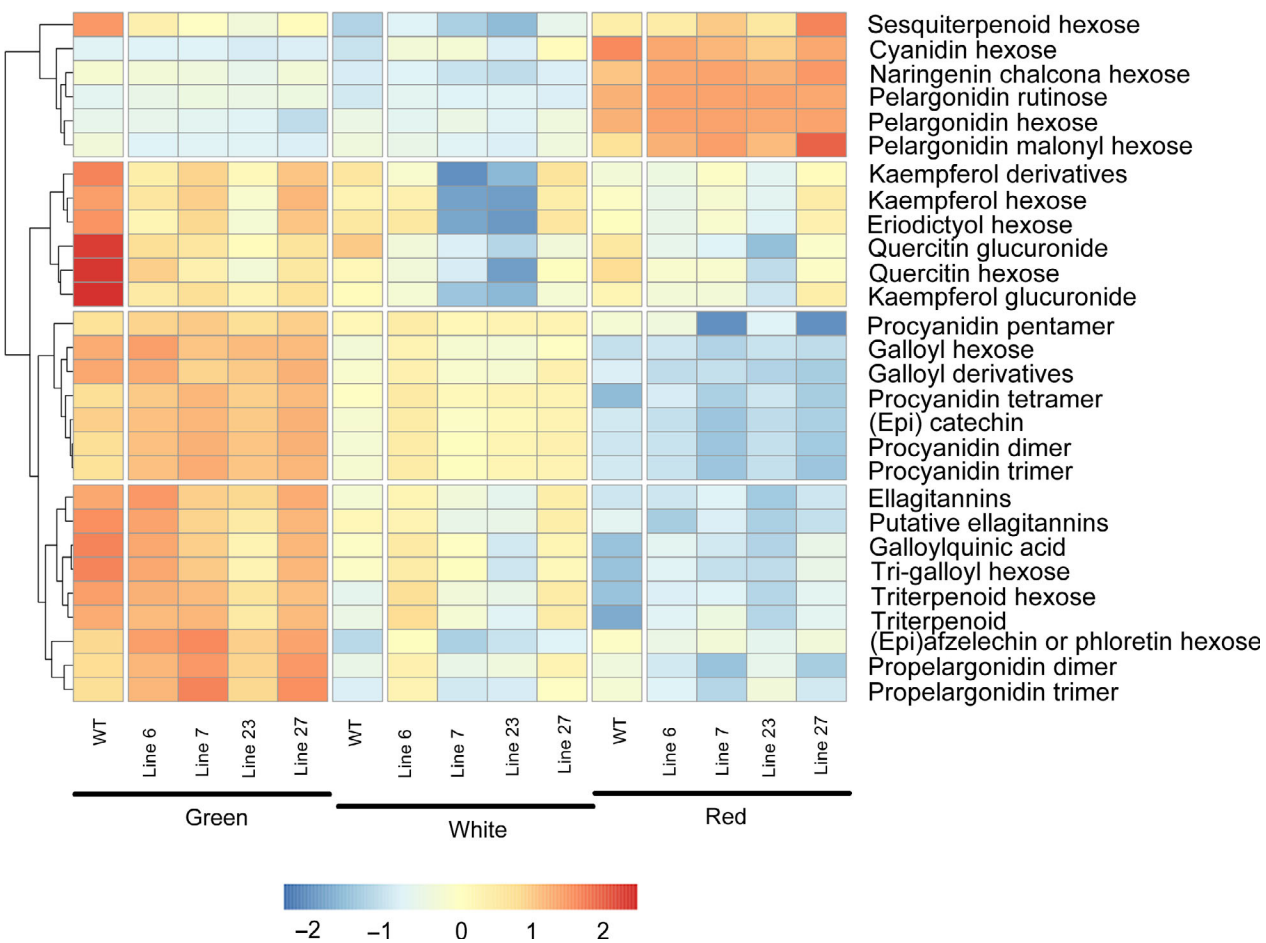

Figure 4 Heat map of identified secondary metabolites in *FaMADS9*-silenced lines and WT strawberry at different developmental stages. A colour-coded matrix represents the mean values of the metabolite intensity which has been $\log_{10}$-transformed and mean-centred.

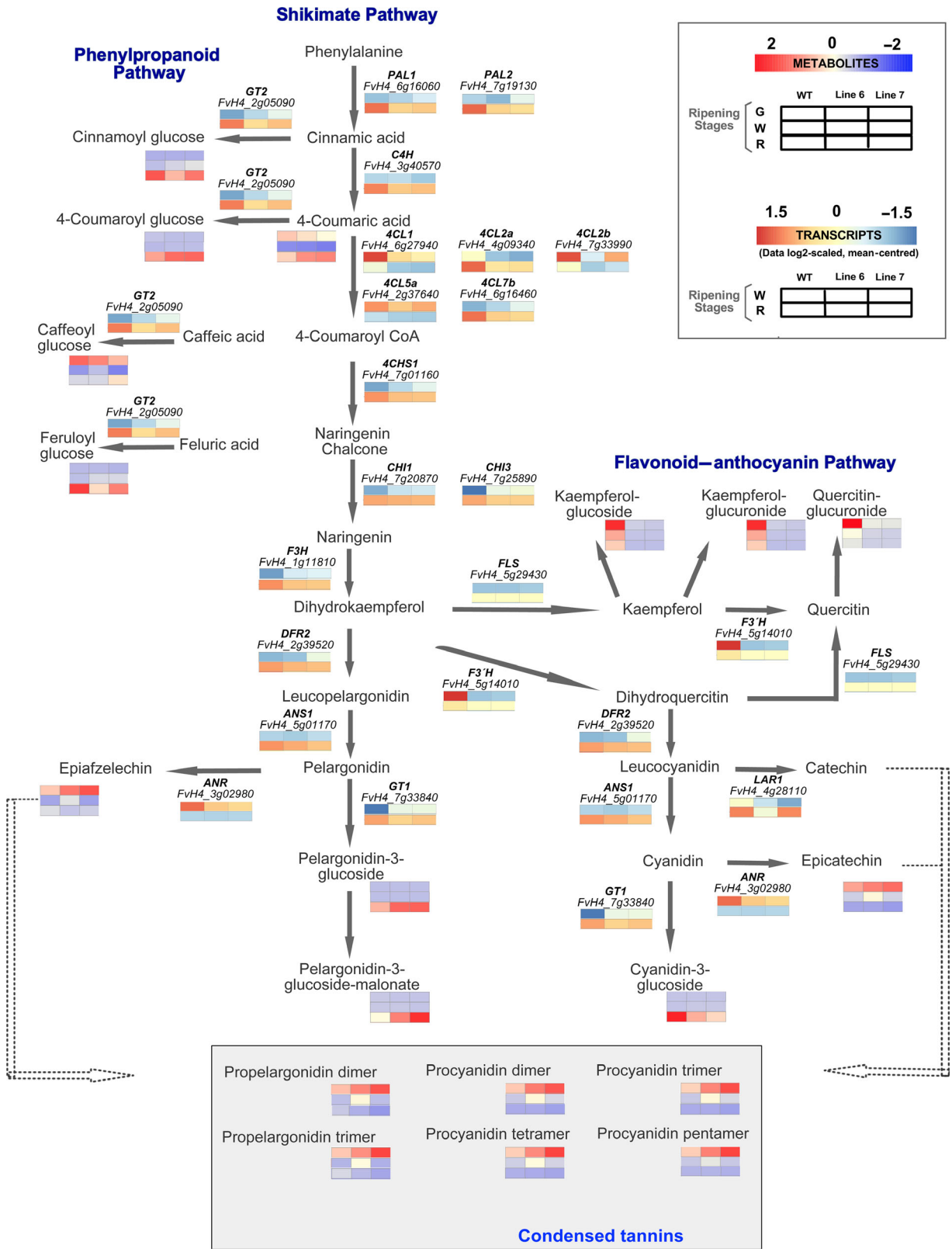

Figure 5 Pathway analysis of genes and enzymes involved in shikimate, phenylpropanoid and flavonoid–anthocyanin pathways. The heat maps represent the transcript (garnet-green) and metabolites (red-blue) data $\log_2$-scaled and mean-centred. *FaANS*, anthocyanidin synthase; *FaANR*, anthocyanidin reductase; *FaCA4H*, cinnamic acid 4-hydroxylase; *FaCHI*, chalcone isomerase; FaCHS, chalcone synthase; *Fa4CL*, 4-coumaroyl-CoA ligase; *FaDFR*, dihydroflavonol reductase; *FaFGT*, flavonoid glucosyltransferase; *FaF3H*, flavanone 3-hydroxylase; *FaF3′H*, flavonoid 3′-hydroxylase; FaFLS, flavonol synthase; *FaGT1*, anthocyanidin glucosyltransferase; *FaGT2*, (hydroxy)cinnamic acid and (hydroxy)benzoic acid glucosyltransferase; *FaPAL*, phenylalanine ammonia lyase. Reactions that have not been fully elucidated are indicated with dotted lines.

transcriptional data (de Luis Balaguer and Sozzani, 2017). The genes selected for the analysis corresponded to 685 genes that were significantly differentially expressed in the receptacle of the *FaMADS9*-silenced fruits at both the white and red stages (Table S2). To infer the relationships among these genes, a transcriptional data set obtained from RNAseq of ripening receptacles at four stages (green, white, turning and red; Sánchez-Sevilla *et al.*, 2017) was used. Previous to the analysis by GENIST, a clustering step was performed on the 685 selected genes using the RNAseq data of the *FaMADS9*-silenced receptacles (Table S1). The GENIST output is shown in Table S15. *FaMADS9* is included in one of the five main clusters, which predicted 44 targets (Table S15). Analysis of the *FaMADS9* subnetwork (Figure 6a) shows connections to four regulatory genes, namely *FvH4_7g12810* (*TCP9*), *FvH4_2g11150* (*GTE7*), *FvH4_7g01060* (*ZFN2*) and *FvH4_5g17780* (*KAN1*), with the last two exhibited a two-way arrangement. *FaMADS9* shared 27 targets with *KAN1*, including *GTE7*, and 17 targets with *ZFN2* (Table S15). GO analysis of the inferred *FaMADS9* targets showed a prevalence of genes associated with primary energetic metabolism (Table S16).

Identification of the FaMADS9-binding DNA sequence

MADS-box proteins are transcription factors that bind DNA via their MADS domains. All MADS proteins recognize a similar consensus sequence in their target genes ($CC(A/T)_6GG$) that has been called the CArG box ($A_{(R)}$ for A rich) (Pellegrini *et al.*, 1995; Santelli and Richmond, 2000). Although CArG boxes are similar, they are not identical, thus conferring specificity to different MADS transcription factors (Aerts *et al.*, 2018). To determine the DNA sequence to which FaMADS9 binds, we employed a protein-binding microarray (PBM11) (Godoy *et al.*, 2011). *FaMADS9* cDNA was fused to MBP and used to hybridize a microarray that contained all possible combinations of 11-mer oligonucleotides. FaMADS9 bound the sequences containing CCAAAAAAAT (Figure 6b) which is highly similar to a CArG.

Analysis of the 1-kb promoter of the *F. vesca* genes corresponding to the putative *FaMADS9* targets inferred from the GRN showed that the *FaMADS9* CArG box was present in 73% of the genes (Table S17). This value is significantly higher than that obtained for a random sample of *F. vesca* genes.

Discussion

Genetic mutants associated with tomato fruit development and ripening have facilitated the identification of numerous candidate genes that can be tested as functional homologues in other fruit species. These genes include the ripening-associated transcription factor *RIN*, which encodes a SEPALLATA MADS-box gene (Vrebalov *et al.*, 2002). The RIN transcription factor has long been believed to be necessary for the induction of ripening (Giovannoni, 2007; Vrebalov *et al.*, 2002). However, a recent study based on an RIN knockout mutant demonstrated that tomato fruit ripening is initiated without *RIN*, even though RIN activity is required for the completion of ripening (Ito *et al.*, 2017). In strawberry, the antisense down-regulation of *FaMADS9*, a putative orthologue of the *RIN* gene, resulted in drastic changes in fruit morphology and firmness, colour development, and gene expression, including the repression of three *MADS* genes (Seymour *et al.*, 2011). Here, we complement this study with the generation and in-depth analysis of four independent *FaMADS9*-silenced strawberry transgenic lines. In our study, the specificity of the transgene silencing is supported by the fact that only the expression of *FaMADS9* among the 34 *MADS* genes expressed during fruit development was down-regulated in red receptacles. The discrepancies found in the phenotype of transgenic fruits in relation to the previous work (Seymour *et al.*, 2011) can be explained by the highly specific silencing of *FaMADS9* achieved here, as supported by the RNAseq data. Silencing of *FaMADS9* in the previous work (Seymour *et al.*, 2011) was performed by 5′-antisense down-regulation, and in addition to *FaMADS9*, three *MADS-box* genes were down-regulated (*FvH4_4g23530*, *FvH4_6g37880* and *FvH4_7g12670*). Here, we found that there was no change in the expression of the *FvH4_4g23530* and *FvH4_7g12670* genes, while the gene *FvH4_6g37880* was up-regulated. This gene corresponds to a *SHATTERPROOF-like* gene that is involved in some processes associated with strawberry fruit ripening (Daminato *et al.*, 2013). Thus, differences in the off-target or downstream effects of the silencing process, as well as in the cultivars, could explain the discrepancies between the two studies.

FaMADS9 is involved in specific developmental processes at the green stage

A previous study of *FaMADS9* expression in strawberry fruits showed the highest expression in the receptacles, with peaks observed at the green and red stages and diminished values observed at the white and turning stages (Sánchez-Sevilla *et al.*, 2017). The generation of *FaMADS9*-specific silenced lines and exhaustive analysis of the transcriptomic and metabolic changes in transformed receptacle have allowed the identification of the developmental processes in which this gene is involved. The elevated number of differentially expressed genes, 2670 genes at the white stage and 1943 at the red stage, is indicative of the central role played by this transcription factor in the growth and ripening of the receptacles of the strawberry fruit. Global analysis of the transcriptomic and metabolomic data shows that, as expected from the *FaMADS9* expression pattern in the fruit, significant changes occurred at the green and red stages.

The green stage is characterized by active cell division that must be supported by the continuous supply of building blocks for the cell structure and composition and the activity of biosynthetic processes. Thus, it has been reported that in strawberry, starch accumulates extremely early in the fruit formation process, while starch degradation predominates during fruit growth and development (Souleyre *et al.*, 2004). These changes in starch levels are correlated with the dramatic decrease in the levels of maltose and isomaltose, the products of starch degradation, during receptacle ripening (Fait *et al.*, 2008). Our finding of altered levels of maltose and isomaltose in the *FaMADS9*-silenced fruits could indicate that the silencing of this gene disrupts the readiness of the fruit to degrade starch in order to fuel growth and ripening. This finding is consistent with earlier work on a tomato *rin* mutant, which indicated the importance of *RIN* in starch synthesis during early fruit development (Osorio *et al.*, 2011). The changes reported here for the galactonic acid-1,4-lactone content are also indicative of the involvement of *FaMADS9* in the growth processes occurring in green receptacles. Strawberry fruit is rich in L-ascorbic acid, which is feasibly involved in the maintenance of the redox buffering capacity during developmental processes (Foyer, 2015). In the green receptacle, ascorbate is likely synthesized via the L-galactose pathway (Cruz-Rus *et al.*, 2011). Although we were unable to detect L-ascorbic acid in the primary chromatograms from the red

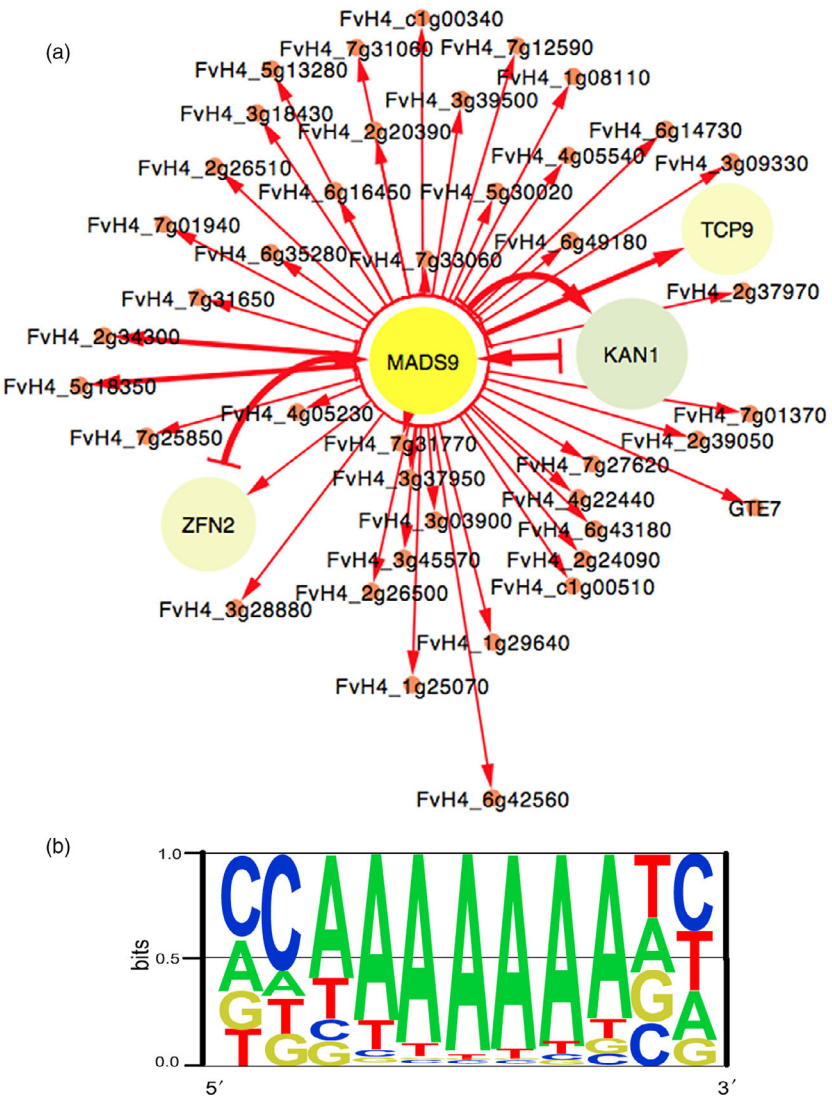

Figure 6 (a) Representation of the *FaMADS9* subnetwork within the gene regulatory network (GRN). Node sizes reflect the number of targets that are inferred. (b) The consensus CArG sequence of FAMADS9 binding to DNA.

receptacle, we found a significant decrease in the level of galactonic acid-1,4-lactone, the final precursor of the biosynthesis pathway in the transgenic green receptacles. Additionally, flavonoids are actively synthesized in strawberry fruits with a stage-specific pattern, with proanthocyanidins and flavonol derivatives being highly abundant at the green stage (Fait *et al.*, 2008). Our in-depth analysis of secondary metabolites in the green receptacles of the silenced lines showed significant changes in these compounds. Taken together, these results reinforce the previously postulated view that the *FaMADS9* gene plays a crucial regulatory role in early fruit development (Seymour *et al.*, 2011).

Whole-transcriptome analysis facilitates the elucidation of the underlying molecular mechanisms supporting the stage and composition of the sample under study. Although our RNAseq analysis was not performed in green receptacles, the results obtained in white receptacles might be indicative of the transcript levels at the green stage. The white stage of strawberry fruit represents the final phase of the growing period and is preliminary to the ripening period. MapMan analysis of the enriched categories within the differentially expressed genes at the white stage also supports the role indicated above for *FaMADS9* at the early developmental stage, which is the case for the highly represented UDP-glucosyl/glucuronosyl transferases. These enzymes are involved in the synthesis of a great diversity of substrates (Caputi *et al.*, 2012), with some of these enzymes participating in the synthesis of structural glucans (Iwai *et al.*, 2002). Additionally, the number of intrinsic membrane proteins down-regulated in the transgenic receptacles delimits the function of *FaMADS9*. The relationship between water movement and fruit growth and ripening has been widely studied (Fouquet *et al.*, 2008). Aquaporins belong to the family of integral membrane channel proteins and play an important role in water homeostasis in plants. In strawberry fruit, it has been reported that a *FaNIP1-1* gene, positively regulated by abscisic acid and negatively regulated by auxins, is active in water transport in the fruit (Molina-Hidalgo, *et al.*, 2015). The only *NIP1-1* gene that was differentially expressed in the present study was up-regulated at the white stage. Transcription analysis in the white receptacles would also explain the decrease in the level of galactonic acid-1,4-lactone, the final intermediate in the ascorbate biosynthesis pathway, in the transgenic green receptacles. This decrease was correlated with down-regulation in the expression of the *mannose-1-phosphate guanyltransferase* (*VTC1*) and *GDP-L-galactose phosphorylase* (*VTC2*)

genes, which encode key regulatory enzymes of ascorbate biosynthesis (Bulley and Laing, 2016).

Effects of *FaMADS9* on specific processes associated with receptacle ripening

One of the most evident ripening-related changes in strawberry fruit is the progressive and extensive loss of firmness, resulting in part from cell wall disassembly (Brummell, 2006; Vicente *et al.*, 2007). In strawberry, these processes were not altered after *FaMADS9* silencing because fruit firmness was not changed in transgenic fruits, nor was the expression of cell wall degrading enzymes such as PLA, PLB and RGlyase in the red stage (Benítez-Burraco *et al.*, 2003; Jiménez-Bermúdez *et al.*, 2002; Molina-Hidalgo *et al.*, 2013; Quesada *et al.*, 2009). Up-regulation of *PG1* and *PG2* genes has no apparent effect on the firmness of the red fruits. This finding excludes a role for *FaMADS9* in normal ripening-related cell wall degradation. However, this result was in direct contrast to the *rin* tomato mutant, which exhibited down-regulation of ripening-related wall metabolism genes (Osorio *et al.*, 2011).

Formation of the cuticle, which is the lipophilic layer that covers the outer epidermal cell wall of the aerial parts of higher plants (Jeffree, 2006), has been described as an important process during fruit ripening (Jeffree, 2006; Nawrath, 2006). In tomato fruit, the cuticle of the *rin* mutant has been described to have a lipid composition that differs from that of normal fruit, which impacts development throughout ripening (Kosma *et al.*, 2010). Similarly, we found differences in the lipid composition of the cuticular wax of *FaMADS9*-silenced fruit. Repression of the regulatory genes *SHN1/WIN1* and *SHNE3*, the latter of which is the closest homolog to the tomato *SlSHN3* (Shi *et al.*, 2013), in the transgenic receptacles would indicate a role for *FaMADS9* in this key aspect of the fruit ripening process. Moreover, the putative *cutin synthase* gene *FaCD1*, mostly expressed in the epidermal layer, was down-regulated in the transgenic receptacle, which suggested that cutin composition and structure must also be altered.

With respect to the changes in flavonoid content in the *FaMADS9*-silenced receptacles, we observed changes in metabolites that were limited to the most abundant condensed tannins, flavonols and anthocyanins. Some metabolic differences were accompanied by corresponding transcriptional changes. Thus, changes in the levels of flavonols and cyanidin-hexoses were correlated with the down-regulation of the flavonoid 3′-hydroxylase gene (*F3′H*) in *FaMADS9*-silenced receptacles. However, changes in the levels of other metabolites were not correlated with changes in the levels of transcripts of genes encoding metabolic enzymes. This finding may suggest that in these cases, the metabolic changes are likely due to the adjustment of metabolic fluxes in response to primary changes in other steps of the pathway. Secondary redirection of the flavonoid metabolism in strawberry fruits has been reported after a primarily induced change in the expression of a specific gene (Fischer *et al.*, 2013).

The involvement of *FaMADS9* in the regulatory system of flavonoid metabolism in the receptacles is supported by the number of TFs, previously reported to participate in the control of the pathway, the expression of which was altered in the *FaMADS9*-silenced lines. These genes included *MYB10* (*FvH4_1g22020*), *PCF1* (*FvH4_6g16170*), *DIV* (*FvH4_6g11950*), *ZFN1* (*FvH4_6g00570*) and *ZFN2* (*FvH4_7g01060*) (Pillet *et al.*, 2015). The complex interaction among these regulatory genes in relation to flavonoid biosynthesis, as well as other developmental changes in ripening receptacles, requires the global analysis of available data sets associated with the process.

Involvement of hormones in the action of *FaMADS9* on strawberry receptacle ripening

The numerous metabolic and transcriptional changes found after the specific silencing of *FaMADS9*, despite the apparent lack of visual changes, point to an involvement of this gene product in the regulatory machinery governing strawberry fruit ripening. Most of the hormones have been reported to participate in strawberry fruit development and ripening (Chai *et al.*, 2013; Csukasi *et al.*, 2011; Estrada-Johnson *et al.*, 2017; Jia *et al.*, 2011; Merchante *et al.*, 2013; Mezzetti *et al.*, 2004), and they are expected to play a main role in the regulation of the process. However, the interplay between hormones and regulatory genes has scarcely been addressed (Csukasi *et al.*, 2012; Vallarino *et al.*, 2015). Here, we found that silencing of *FaMADS9* causes changes in the expression of an elevated number of *ARFs* but also a drastic reduction in the expression of ABA-synthesizing genes such as *FaNCED1*, *FaNCED2* and *FaNCED3* in the transgenic receptacles, and a subsequent decrease in AB*A* content. Silencing of *FaNCED1* and *FaNCED2* was observed in *FaGAMYB*-silenced receptacles (Vallarino *et al.*, 2015), as well as reduced levels of ABA in the transgenic tissue. Notably, the *ASR* gene (*FvH4_2g13410*), which is involved in the ABA transduction pathway, was up-regulated in red receptacles. This gene has been reported to play a key role in strawberry fruit ripening (Jia *et al.*, 2016). On the other hand, the ABA-negative regulator *SnRK2.6* (*FvH4_2g06910*), which is also involved in the regulation of strawberry fruit ripening (Han *et al.*, 2015), was up-regulated in white receptacle. All these results point to a drastic change in ABA signalling in the *FaMADS9*-silenced receptacle from early stages of fruit development. Particularly interesting is the *SHP* gene, the only *MADS* up-regulated in the transgenic receptacle, as this gene has been reported to play a main role in strawberry fruit ripening, and the expression of this gene is antagonistically regulated by auxin and ABA (Daminato *et al.*, 2013).

The inference of gene regulatory networks (GRNs) has been proposed as a method for identifying candidate genes from large-scale data sets. This method uses transcriptional data as input and produces an inferred network showing the most likely regulatory pathways of the genes of interest based on the data. The availability of time course data allowed us to infer directed networks based on dynamic Bayesian networks (de Luis Balaguer *et al.*, 2017) that infer statistical dependence among selected genes. Here, applied to the DE genes in the white and red stages of *FaMADS9*-silenced receptacles, this method provided a subnetwork centred around *FaMADS9* with connections to different regulatory genes. The presence of the FaMADS9 DNA-binding sequence in the promoters of the corresponding F. vesca genes further supports to a possible direct interaction between *FaMADS9* and the inferred targets, some of them consistent with the additional information provided in the present publication. Thus, the *KAN1* gene has been reported to act in Arabidopsis as a transcriptional repressor of genes in the auxin action pathway (Huang *et al.*, 2014), whereas the *ZFN2* and *DIV* genes have been linked to anthocyanin biosynthesis in strawberry fruit (Pillet *et al.*, 2015). Other predicted targets, such as *GTE7*, belong to a family of transcription factors that mediate ABA and sugar response in Arabidopsis (Misra *et al.*, 2018).

In summary, our transcriptomic and metabolomic studies on the receptacles of strawberry transgenic lines, in which the SEPALLATA MADS-box gene *FaMADS9* was silenced, reveal that this gene is integrated into the regulatory network controlling the ripening of this non-climacteric fruit. Furthermore, this role was extended to the growth of the receptacles at early developmental stages. As was recently reported for the putative *RIN* orthologue in tomato fruit, *FaMADS9* is not a general regulator but is involved in specific developmental changes that occur during strawberry ripening, some of which are relevant for fruit quality parameters such as the Brix index, the flavonoid content and the composition of the cuticle waxes. Additionally, we were able to draw several important conclusions regarding transcriptomic/metabolomic regulation during strawberry ripening, thus providing new insights into the regulatory network underlying strawberry fruit ripening. However, the inference of the GRN and the presence of FaMADS9 DNA-binding sequence in the inferred targets do not proof a direct interaction between them. Thus, a transactivation assay should confirm this possibility.

Experimental Procedures

Plant material and sampling

Silencing of *FaMADS9* (GenBank AF484683) was performed in *Fragaria x anannasa* Duch cv. Camarosa. Given the high sequence similarity between different members of the MADS-box gene family, the fragment chosen for silencing was located in the C-terminal domain, which is the most divergent between MADS genes (primers listed in Table S18). The construct for the post-transcriptional silencing (*FaMADS9*-RNAi) was generated from a 241 bp fragment of *FaMADS9* from cv. Camarosa and cloned into pHANNIBAL. Then, it was cut with *Spe*I/*Sac*I and cloned in *Xba*I/*Sac*I sites of pBINplus binary vector. Strawberry plants were transformed as previously described by El-Mansouri *et al.*, (1996). The fruits were harvested at three different developmental stages: green, G; white, W; and red, R. Transcriptome and metabolomic analyses were performed in three separate pools of 20–25 fruits each. Each pool was from three different plants. These biological replicates came from 9 transgenic and wild-type plants (all of which were grown in the greenhouse; the genotypes were randomly distributed). All fruits were frozen immediately in liquid nitrogen, and achenes were removed using a scalpel on frozen fruits.

RNA extraction and transcriptome analysis by RNAseq

Total RNA was extracted as previously reported (Vallarino *et al.*, 2015). RNA integrity was verified using the 2100 Bioanalyzer (Agilent Technologies, Santa Clara, CA), and RNA integrity number (RIN) values were >8 for all biological replicates. Expression analysis by RNAseq of transgenic lines (L6 and L7) and WT was performed in triplicate RNA from receptacle tissue in two development stages (white and red). Libraries preparation, sequencing and mapping were performed as previously described (Sánchez-Sevilla *et al.*, 2017). Normalized RNAseq fragment counts were used to measure the relative abundances of transcripts expressed as fragments per kilobase of exon per million fragments mapped (FPKM). For assignment of functional gene predictions, MapMan 'BINs' (Lohse *et al.*, 2014) and open-source *F. vesca* gene ontology (GO) annotation (Darwish *et al.*, 2015; Edger *et al.*, 2018; Shulaev *et al.*, 2011) were used. RNAseq raw data are available under http://www.ebi.ac.uk/ena/data/view/PRJEB32676.

Gene expression analysis by quantitative real-time PCR (qRT-PCR)

Total RNA was extracted as described previously for the transcriptome analysis. These biological replicates were different from those used for transcriptome analysis. Expression data were normalized to the reference genes *actin* and *glyceraldehyde-3-phosphate dehydrogenase* (*GADPH*), with comparable results. Values showed in this publication are normalized to *GADPH* (Salvatierra *et al.*, 2010). Primers are listed in Table S18.

Extraction and analysis of polar metabolites using GC-MS and UPLC-Orbitrap-MS/MS

Primary metabolite profiles and ABA were obtained by GC-time of flight-(TOF)-MS from the same material as used for transcriptome analysis. Metabolite extraction, derivatization and analysis were determined as described by Osorio *et al.* (2012). Secondary metabolite analysis system was performed using method described by Vallarino *et al.* (2018) by Waters Acquity UPLC. Full documentation of metabolite profiling data acquisition and interpretation is provided in Table S14.

Wax analysis

A protocol based on Yeats *et al.* (2012b) was used for wax analysis.

DNA-binding domain

Identification of the FaMADS9 DNA-binding motif and statistical analysis was performed as in Berger and Bulyk (2009) with the exception that the cDNA of *FaMADS9* was fused to MBP (Maltose binding protein). The consensus logo was done with the use of the enoLOGOS server (http://lagavulin.ccbb.pitt.edu/cgi-bin/enologos/enologos.cgi).

Promoter analysis for the detection of putative transcription factor binding sites was performed on the PlantPAN3.0 resource (http://plantpan.itps.ncku.edu.tw/index.html), developed by Chow *et al.* (2019).

Gene regulatory network

To deduce the GRN, a set of 685 genes that were significantly differentially expressed in the receptacle of the *FaMADS9*-silenced fruits compared to the untransformed fruits, both at white and red stages, were selected. For this set of genes, a computational pipeline (GENIST) (de Luis Balaguer *et al.*, 2017) was used to infer their relationships from a combination of spatial (achene, receptacle and leaf) and temporal (green; white; turning; red) transcriptional data obtained by RNAseq (Sánchez-Sevilla *et al.*, 2017). Clustering of genes before the inference step by GENIST has been shown to improve GENIST performance (de Luis Balaguer *et al.*, 2017), since it reduces the complexity of the inference steps for large networks. Therefore, a clustering step was performed previous to inference by GENIST. The clustering data here used were the RNAseq expression data obtained from the receptacle of control and *FaMADS9*-silenced fruits, at white and red stages (Table S1). Application of GENIST was performed as previously reported (de Luis Balaguer *et al.*, 2017).

Acknowledgements

This work was supported by grants BIO2013-44199-R, AGR12-40066-CO2-02, and RTI2018-099797-B-100 (MINECO, Spain), and the European Union's H2020 Programme (GoodBerry; grant

number 679303) and ERC-2014-StG638134. DP and SO acknowledge the support by Spanish Ministry of Science and Innovation (Ramón and Cajal contracts, RYC2011-09170 and RYC2013-12699).

Conflicts of interest

The authors declare no conflict of interest.

Author contributions

V.V. and S.O. coordinated the analysis of the data and prepared the manuscript. J.G.V. and S.O. performed the evaluation, characterization and metabolomic analysis of the transgenic lines. C.M cloned the gene and made the initial expression analysis. C.M and A.C. made the *FaMADS9*-RNAi silencing constructs and generated the transgenic lines. C.M., A.C and M.T.A performed the preliminary characterizations of the transgenic lines. A.V. made the expression analyses that involved different parts of the receptacle. I.A., D.P., MAB and J.F.S-S performed the analysis of the RNAseq data. M.A.dL.B., R.S. and V.V. made the GRN. L.W. and A.R.F performed the metabolomic analysis. R.S. performed the DNA-binding domain experiment. J.J.G made the RNAseq experiment**.** All authors participated and reviewed the writing of the manuscript.

References

Aerts, N., de Bruijn, S., van Mourik, H., Angenent, G.C. and van Dijk, A.D.J. (2018) Comparative analysis of binding patterns of MADS-domain proteins in Arabidopsis thaliana. *BMC Plant Biol.* **18**, 131.

Aharoni, A. and O'Connell, A.P. (2002) Gene expression analysis of strawberry achene and receptacle maturation using DNA microarrays. *J. Exp. Bot.* **53**, 2073–2087.

Aharoni, A., De Vos, C.H., Wein, M., Sun, Z., Greco, R., Kroon, A., Mol, J.N. *et al.* (2001) The strawberry *FaMYB1* transcription factor suppresses anthocyanin and flavonol accumulation in transgenic tobacco. *Plant J.* **28**, 319–332.

Aharoni, A., Dixit, S., Jetter, R., Thoenes, E., van Arkel, G. and Pereira, A. (2004) The SHINE clade of AP2 domain transcription factors activates wax biosynthesis, alters cuticle properties, and confers drought tolerance when overexpressed in Arabidopsis. *Plant Cell*, **16**, 2463–2480.

Aragüez, I., Osorio, S., Hoffmann, T., Rambla, J.L., Medina-Escobar, N., Granell, A., Botella, M.A. *et al.* (2013) Eugenol production in achenes and receptacles of strawberry fruits is catalysed by synthases exhibiting distinct kinetics. *Plant Physiol.* **163**, 946–958.

Benítez-Burraco, A., Blanco-Portales, R., Redondo-Nevado, J., Bellido, M.L., Moyano, E., Caballero, J.L. and Muñoz-Blanco, J. (2003) Cloning and characterization of two ripening-related strawberry (*Fragaria x ananassa* cv. Chandler) pectate lyase genes. *J. Exp. Bot.* **54**, 633–645.

Berger, M.F. and Bulyk, M.L. (2009) Universal protein-binding microarrays for the comprehensive characterization of the DNA-binding specificities of transcription factors. *Nat. Protoc.* **4**, 393–411.

Bernard, A. and Joubès, J. (2013) Arabidopsis cuticular waxes: Advances in synthesis, export and regulation. *Prog. Lipid. Res.* **52**, 110–129.

Brummell, D.A. (2006) Cell wall disassembly in ripening fruit. *Funct. Plant Biol.* **33**, 103–119.

Bulley, S. and Laing, W. (2016) The regulation of ascorbate biosynthesis. *Curr. Opin. Plant Biol.* **33**, 15–22.

Caputi, J., Malnoy, M., Goremykin, V., Nikiforova, S. and Martens, S. (2012) A genome-wide phylogenetic reconstruction of family 1 UDP-glycosyltransferases revealed the expansion of the family during the adaptation of plants to life on land. *Plant J.* **69**, 1030–1042.

Chai, Y.M., Jia, H.F., Li, C.L., Dong, Q.H. and Shen, Y.Y. (2011) FaPYR1 is involved in strawberry fruit ripening. *J. Exp. Bot.* **62**, 5079–5089.

Chai, Y.M., Zhang, Q., Tian, L., Li, C.L., Xing, Y., Qin, L. and Shen, Y.Y. (2013) Brassinosteroid is involved in strawberry fruit ripening. *Plant Growth Regul.* **69**, 63–69.

Chow, C.N., Lee, T.Y., Hung, Y.C., Li, G.Z., Tseng, K.C., Liu, Y.H., Kuo, P.L. *et al.* (2019) PlantPAN3.0: a new and updated resource for reconstructing transcriptional regulatory networks from ChIP-seq experiments in plants. *Nucleic. Acids Res.* **47**(D1), D1155–D1163.

Concha, C.M., Figueroa, N.E., Poblete, L.A., Oñate, F.A., Schwab, W. and Figueroa, C.R. (2013) Methyl jasmonate treatment induces changes in fruit ripening by modifying the expression of several ripening genes in *Fragaria chiloensis* fruit. *Plant Physiol. Biochem.* **70**, 433–444.

Cruz-Rus, E., Amaya, I., Sánchez-Sevilla, J.F., Botella, M.A. and Valpuesta, V. (2011) Regulation of L-ascorbic acid content in strawberry fruit. *J. Exp. Bot.* **62**, 4191–4201.

Csukasi, F., Osorio, S., Gutierrez, J.R., Kitamura, J., Giavalisco, P., Nakajima, M., Fernie, A.R. *et al.* (2011) Gibberellin biosynthesis and signalling during development of the strawberry receptacle. *New Phytol.* **191**, 376–390.

Csukasi, F., Donaire, L., Casañal, A., Martínez-Priego, L., Botella, M.A., Medina-Escobar, N., Llave, C. *et al.* (2012) Two strawberry miR159 family members display developmental specific expression patterns in the fruit receptacle and cooperatively regulate *Fa-GAMYB*. *New Phytol.* **195**, 47–57.

Daminato, M., Guzzo, F. and Casadoro, G. (2013) A SHATTERPROOF-like gene controls ripening in non-climacteric strawberries, and auxin and abscisic acid antagonistically affect its expression. *J. Exp. Bot.* **64**, 3775–3786.

Darwish, O., Shahan, R., Liu, Z., Slovin, J.P. and Alkharouf, N.W. (2015) Re-annotation of the woodland strawberry (*Fragaria vesca*) genome. *BMC Genom.* **16**, 29.

Domínguez, E., Heredia-Guerrero, J.A. and Heredia, A. (2015) Plant cutin genesis: unanswered questions. *Trends Plant Sci.* **20**, 551–558.

Edger, P.P., VanBuren, R., Colle, M., Poorten, T.J., Wai, C.M., Niederhuth, C.E., Alger, E.I. *et al.* (2018) Single-molecule sequencing and optical mapping yields an improved genome of woodland strawberry (*Fragaria vesca*) with chromosome-scale contiguity. *GigaScience*, **7**, 1–7.

Elitzur, T., Vrebalov, J., Giovannoni, J.J., Goldschmidt, E.E. and Friedman, H. (2010) The regulation of MADS-box gene expression during ripening of banana and their regulatory interaction with ethylene. *J. Exp. Bot.* **61**, 1523–1535.

El-Mansouri, I., Mercado, J.A., Valpuesta, V., López-Aranda, J.M., Pliego, F. and Quesada, M.A. (1996) Shoot regeneration and Agrobacterium mediated transformation of *Fragaria vesca* L. *Plant Cell. Rep.* **15**, 642–646.

Estrada-Johnson, E., Csukasi, F., Pizarro, C.M., Vallarino, J.G., Kiryakova, Y., Vioque, A., Merchante, C. *et al.* (2017) Transcriptome analysis in strawberry fruits reveals active auxin biosynthesis and signaling in the ripe receptacle. *Front. Plant Sci.* **8**, 889.

Fait, A., Hanhineva, K., Beleggia, R., Dai, N., Rogachev, I., Nikiforova, V.J., Fernie, A.R. *et al.* (2008) Reconfiguration of achene and receptacle metabolic networks during strawberry fruit development. *Plant Physiol.* **148**, 730–750.

Fischer, T.C., Mirbeth, B., Rentsch, J., Sutter, C., Ring, L., Flachowsky, H., Habegger, R. *et al.* (2013) Premature and ectopic anthocyanin formation by silencing of anthocyanidin reductase in strawberry (*Fragaria* × *ananassa*). *New Phytol.* **201**, 440–451.

Fouquet, R., León, C., Ollat, N. and Barrieu, F. (2008) Identification of grapevine aquaporins and expression analysis in developing berries. *Plant Cell Rep.* **27**, 1541–1550.

Foyer, C.H. (2015) Redox homeostasis: Opening up ascorbate transport. *Nat. Plants,* **1**, 14012.

Giovannoni, J.J. (2007) Fruit ripening mutants yield insights into ripening control. *Curr. Opin. Plant Biol.* **10**, 283–289.

Godoy, M., Franco-Zorrilla, J.M., Pérez-Pérez, J., Oliveros, J.C., Lorenzo, O. and Solano, R. (2011) Improved protein-binding microarrays for the identification of DNA-binding specificities of transcription factors. *Plant J.* **66**, 700–711.

Han, J.Y., Kim, M.J., Ban, Y.W., Hwang, H.S. and Choi, Y.E. (2013) The involvement of β-amyrin 28-oxidase (CYP716A52v2) in oleanane-type ginsenoside biosynthesis in Panax ginseng. *Plant Cell Physiol.* **54**(12), 2034.2046.

Han, Y., Dang, R., Li, J., Jiang, J., Zhang, N., Jia, M., Wei, L. *et al.* (2015) SUCROSE NONFERMENTING1-RELATED PROTEIN KINASE2.6, an ortholog of OPEN STOMATA1, is a negative regulator of strawberry fruit development and ripening. *Plant Physiol.* **167**, 915–930.

Härtl, K., Denton, A., Franz-Oberdorf, K., Hoffmann, T., Spornraft, M., Usadel, B. and Schwab, W. (2017) Early metabolic and transcriptional variations in fruit of natural white-fruited *Fragaria vesca* genotypes. *Sci. Rep.* **7**, 45113.

Huang, T., Harrar, Y., Lin, C., Reinhart, B., Newell, N.R., Talavera-Rauh, F., Hokin, S.A. *et al.* (2014) Arabidopsis KANADI1 Acts as a Transcriptional Repressor by Interacting with a Specific cis-Element and Regulates Auxin Biosynthesis, Transport, and Signaling in Opposition to HD-ZIPIII Factors. *Plant Cell*, **26**, 246–262.

Ito, Y., Nishizawa-Yokoi, A., Endo, M., Mikami, M., Shima, Y., Nakamura, N., Kotake-Nara, E. *et al.* (2017) Re-evaluation of the *rin* mutation and the role of *RIN* in the induction of tomato ripening. *Nat. Plants*, **3**(11), 866–874.

Iwai, H., Masaoka, N., Ishii, T. and Satoh, S. (2002) A pectin glucuronyltransferase gene is essential for intercellular attachment in the plant meristem. *Proc. Natl. Acad. Sci. USA*, **99**(25), 16319–16324.

Jaakola, L., Poole, M., Jones, M.O., Kämäräinen-Karppinen, T., Koskimäki, J.J., Hohtola, A., Häggman, H. *et al.* (2010) A SQUAMOSA MADS box gene involved in the regulation of anthocyanin accumulation in bilberry fruits. *Plant Physiol.* **153**, 1619–1629.

Jeffree, C.E. (2006) The fine structure of the plant cuticle. In *Annual Plant Reviews Volume 23: Biology of the Plant Cuticle*, (Riederer, M. and Müller, C., eds), pp. 11–125. Oxford: Blackwell.

Jia, H., Chai, Y., Li, C., Lu, D., Luo, J., Qin, L. and Shen, Y. (2011) Abscisic acid plays an important role in the regulation of strawberry fruit ripening. *Plant Physiol.* **157**, 188–199.

Jia, H., Jiu, S., Zhang, C., Wang, C., Tariq, P., Liu, Z., Wang, B. *et al.* (2016) Abscisic acid and sucrose regulate tomato and strawberry fruit ripening through the abscisic acid-stress-ripening transcription factor. *Plant Biotechnol. J.* **14**, 2045–2065.

Jiménez-Bermúdez, S., Redondo-Nevado, J., Muñoz-Blanco, J., Caballero, J.L., López-Aranda, J.M., Valpuesta, V., Pliego-Alfaro, F. *et al.* (2002) Manipulation of strawberry fruit softening by antisense expression of a pectate lyase gene. *Plant Physiol.* **128**, 751–759.

Kosma, D.K., Eugene, P., Parsons, E.P., Isaacson, T., Lu, S., Rose, J.K.C. and Jenks, M.A. (2010) Fruit cuticle lipid composition during development in tomato ripening mutants. *Physiol. Plant.* **139**, 107–117.

Lee, S.B. and Suh, M.C. (2015) Advances in the understanding of cuticular waxes in Arabidopsis thaliana and crop species. *Plant Cell Rep.* **34**, 557–572.

Li, D., Li, L., Luo, Z., Mou, W., Mao, L. and Ying, T. (2015) Comparative transcriptome analysis reveals the influence of abscisic acid on the metabolism of pigments, ascorbic acid and folic acid during strawberry fruit ripening. *PLoS ONE*, **10**, e0130037.

Lin-Wang, K., Bolitho, K., Grafton, K., Kortstee, A., Karunairetnam, S., McGhie, T.K., Espley, R.V. *et al.* (2010) An *R2R3 MYB* transcription factor associated with regulation of the anthocyanin biosynthetic pathway in Rosaceae. *BMC Plant Biol.* **10**, 50.

Lohse, M., Nagel, A., Herter, T., May, P., Schroda, M., Zrenner, R., Tohge, T. *et al.* (2014) Mercator: a fast and simple web server for genome scale functional annotation of plant sequence data. *Plant Cell Environ.* **37**, 1250–1258.

de Luis Balaguer, M.A. and Sozzani, R. (2017) Inferring gene regulatory networks in the Arabidopsis root using a dynamic bayesian network approach. *Methods Mol. Biol.* **1629**, 331–348.

de Luis Balaguer, M.A., Fisher, A.P., Clark, N.M., Fernández-Espinosa, M.G., Möller, B.K., Weijers, D., Lohmann, J.U. *et al.* (2017) Predicting gene regulatory networks by combining spatial and temporal gene expression data in Arabidopsis root stem cells. *Proc. Natl. Acad. Sci. USA*, **114**(36), E7632–E7640.

Luo, H., Dai, C., Li, Y., Feng, J., Liu, Z. and Kang, C. (2018) Reduced Anthocyanins in Petioles codes for a GST anthocyanin transporter that is essential for the foliage and fruit coloration in strawberry. *J. Exp. Bot.* **69**, 2595–2608.

Martin, L.B.B., Romero, P., Fich, E.A., Domozych, D.S. and Rose, J.K.C. (2017) Cuticle biosynthesis in tomato leaves is developmentally regulated by abscisic acid. *Plant Physiol.* **174**, 1384–1398.

Medina-Puche, L., Cumplido-Laso, G., Amil-Ruiz, F., Hoffmann, T., Ring, L., Rodríguez-Franco, A., Caballero, J.L. *et al.* (2014) MYB10 plays a major role in the regulation of flavonoid/phenylpropanoid metabolism during ripening of *Fragaria x ananassa* fruits. *J. Exp. Bot.* **65**, 401–417.

Medina-Puche, L., Molina-Hidalgo, F.J., Boersma, M., Schuurink, R.C., López-Vidriero, I., Solano, R., Franco-Zorrilla, J.M. *et al.* (2015) An R2R3-MYB transcription factor regulates eugenol production in ripe strawberry fruit receptacles. *Plant Physiol.* **168**, 598–614.

Merchante, C., Vallarino, J.G., Osorio, S., Aragüez, I., Villarreal, N., Ariza, M.T., Martínez, G.A. *et al.* (2013) Ethylene is involved in strawberry fruit ripening in an organ-specific manner. *J. Exp. Bot.* **64**(14), 4421–4439.

Mezzetti, B., Landi, L., Pandolfini, T. and Spena, A. (2004) The defH9-iaaM auxin-synthesizing gene increases plant fecundity and fruit production in strawberry and raspberry. *BMC Biotech.* **4**, 4.

Misra, A., McKnight, T.D. and Mandadi, K.K. (2018) Bromodomain proteins GTE9 and GTE11 are essential for specific BT2-mediated sugar and ABA responses in *Arabidopsis thaliana*. *Plant Mol. Biol.* **96**(4–5), 393–402.

Molina-Hidalgo, F.J., Franco, A.R., Villatoro, C., Medina-Puche, L., Mercado, J.A., Hidalgo, M.A., Monfot, A. *et al.* (2013) The strawberry (*Fragaria x ananassa*) fruit-specific rhamnogalacturonate lyase 1 (FaRGLyase1) gene encodes an enzyme involved in the degradation of cell-wall middle lamellae. *J. Exp. Bot.* **64**, 1471–1483.

Molina-Hidalgo, F.J., Medina-Puche, L., Gelis, S., Ramos, J., Sabir, F., Soveral, G., Prista, C. *et al.* (2015) Functional characterization of FaNIP1;1 gene, a ripening-related and receptacle-specific aquaporin in strawberry fruit. *Plant Sci.* **238**, 198–211.

Molina-Hidalgo, F.J., Medina-Puche, L., Cañete-Gomez, C.J., Franco-Zorrilla, J.M., López-Vidriero, I., Solano, R., Caballero, J.L. *et al.* (2017) The fruit-specific FaDOF2 transcription factor regulates the production of eugenol in ripen fruit receptacle. *J. Exp. Bot.* **68**, 4529–4543.

Mukkun, L. and Singh, Z. (2009) Methyl jasmonate plays a role in fruit ripening of 'Pajaro' strawberry through stimulation of ethylene biosynthesis. *Sci. Hortic.* **123**, 5–10.

Nawrath, C. (2006) Unraveling the complex network of cuticular structure and function. *Curr. Opin. Plant Biol.* **9**, 281–287.

Nitsch, J. (1950) Growth and morphogenesis of the strawberry as related to auxin. *Am. J. Bot.* **37**, 211–215.

Osorio, S., Bombarely, A., Giavalisco, P., Usadel, B., Stephens, C., Aragüez, I., Medina-Escobar, N. *et al.* (2011) Demethylation of oligogalacturonides by *FaPE1* in the fruits of the wild strawberry *Fragaria vesca* triggers metabolic and transcriptional changes associated with defense and development of the fruit. *J. Exp. Bot.* **62**, 2855–2873.

Osorio, S., Do, P.T. and Fernie, A.R. (2012) Profiling primary metabolites of tomato fruit with gas chromatography/mass spectrometry. *Methods Mol. Biol.* **860**, 101–109.

Pellegrini, L., Tan, S. and Richmond, T.J. (1995) Structure of serum response factor core bound to DNA. *Nature*, **376**, 490–498.

Perkins-Veazie, P. (1995) Growth and ripening of strawberry fruit. *Hortic. Rev.* **17**, 267–297.

Pillet, J., Yu, H.-W., Chambers, A.H., Whitaker, V.M. and Folta, K.M. (2015) Identification of candidate flavonoid pathway genes using transcriptome correlation network analysis in ripe strawberry (Fragaria × ananassa) fruits. *J. Exp. Bot.* **66**, 4455–4467.

Quesada, M.A., Blanco-Portales, R., Posé, S., García-Gago, J.A., Jiménez-Bermúdez, S., Muñoz-Serrano, A., Caballero, J.L. *et al.* (2009) Antisense down-regulation of the FaPG1 gene reveals an unexpected central role for polygalacturonase in strawberry fruit softening. *Plant Physiol.*, **150**, 1022–1032.

Salvatierra, A., Pimentel, P., Moya-Leon, M.A., Caligari, P.D.S. and Herrera, R. (2010) Comparison of transcriptional profiles of flavonoid genes and anthocyanin contents during fruit development of two botanical forms of *Fragaria chiloensis* ssp. *chiloensis*. *Phytochem*, **71**, 1839–1847.

Sánchez-Sevilla, J.F., Vallarino, J.G., Osorio, S., Bombarely, A., Posé, D., Merchante, C., Botella, M.A. *et al.* (2017) Gene expression atlas of fruit ripening and transcriptome assembly from RNA-seq data in octoploid strawberry (*Fragaria* × *ananassa*). *Sci. Rep.* **7**, 13737.

Santelli, E. and Richmond, T.J. (2000) Crystal structure of MEF2A core bound to DNA at 1.5 Å resolution. *J. Mol. Biol.* **29**, 437–449.

Schaart, J., Dubos, C., Romero de la Fuente, I., van Houwelingen, A., De Vos, R., Jonker, H., Xu, W. *et al.* (2013) Identification and characterization of MYB-bHLH-WD40 regulatory complexes controlling proanthocyanidin biosynthesis in strawberry (*Fragaria x ananassa*) fruits. *New Phytol.* **197**, 454–467.

Schulenburg, K., Feller, A., Hoffmann, T., Schecker, J.H., Martens, S. and Schwab, W. (2016) Formation of β-glucogallin, the precursor of ellagic acid in strawberry and raspberry. *J. Exp. Bot.* **67**, 2299–2308.

Seymour, G.B., Ryder, C.D., Cevik, V., Hammond, J.P., Popovich, A., King, G.J., Vrebalov, J. *et al.* (2011) A SEPALLATA gene is involved in the development and ripening of strawberry (*Fragaria x ananassa* Duch.) fruit, a non-climacteric tissue. *J. Exp. Bot.* **62**, 1179–1188.

Shi, J.X., Adato, A., Alkan, N., He, Y., Lashbrooke, J., Matas, A.J., Meir, S. *et al.* (2013) The tomato SlSHINE3 transcription factor regulates fruit cuticle formation and epidermal patterning. *New Phytol.* **197**, 468–480.

Shulaev, V., Sargent, D.J., Crowhurst, R.N., Mockler, T.C., Folkerts, O., Delcher, A.L., Jaiswal, P. *et al.* (2011) The genome of woodland strawberry (*Fragaria vesca*). *Nat Genet.* **43**, 109–116.

Souleyre, E.J.F., Taylor, M., Iannetta, P.P.M., Ross, H.A., Shepherd, L.V.T., Hancock, R., Viola, R. *et al.* (2004) Carbohydrate metabolism in ripening strawberry fruit. *Physiol. Plant.* **121**, 369–376.

Tadiello, A., Pavanello, A., Zanin, D., Caporali, E., Colombo, L., Rotino, G.L., Trainotti, L. *et al.* (2009) A PLENA-like gene of peach is involved in carpel formation and subsequent transformation into a fleshy fruit. *J. Exp. Bot.* **60**, 651–661.

Thimm, O., Bläsing, O., Gibon, Y., Nagel, A., Meyer, S., Krüger, P., Selbig, J. *et al.* (2004) MAPMAN: a user-driven tool to display genomics data sets onto diagrams of metabolic pathways and other biological processes. *Plant J.* **37**, 914–939.

Tranbarger, T.J., Dussert, S., Joët, T., Argout, X., Summo, M., Champion, A., Cros, D. *et al.* (2011) Regulatory mechanisms underlying oil palm fruit mesocarp maturation, ripening, and functional specialization in lipid and carotenoid metabolism. *Plant Physiol.* **156**, 564–584.

Vallarino, J.G., Osorio, S., Bombarely, A., Casañal, A., Cruz-Rus, E., Sánchez-Sevilla, J.F., Amaya, I. *et al.* (2015) Central role of *FaGAMYB* in the transition of strawberry receptacle from development to ripening. *New Phytol.* **208**, 482–496.

Vallarino, J.G., de Abreu e Lima, F., Soria, C., Tong, H., Pott, D.M., Willmitzer, L., Fernie, A.R. *et al.* (2018) Genetic diversity of strawberry germplasm using metabolomic biomarkers. *Sci. Rep.* **8**, 14386.

Valpuesta, V. and Botella, M.A. (2004) Biosynthesis of L-ascorbic acid in plants: New pathways for an old antioxidant. *Trends Plant Sci.* **9**, 573–577.

Vicente, A.R., Saladié, M., Rose, J.K.C. and Labavitch, J.M. (2007) The linkage between cell wall metabolism and the ripening-associated softening of fruits: looking to the future. *J. Sci. Food Agric.* **87**, 1435–1448.

Vrebalov, J., Ruezinsky, D., Padmanabhan, V., White, R., Medrano, D., Drake, R., Schuch, W. *et al.* (2002) A MADS-box gene necessary for fruit ripening at the tomato ripening-inhibitor (rin) locus. *Science*, **296**, 343–346.

Yeats, T.H., Martin, L.B.B., Viart, H.M.F., Isaacson, T., He, Y., Zhao, L., Matas, A.J. *et al.* (2012a) The identification of cutin synthase: formation of the plant polyester cutin. *Nat. Chem. Biol.* **8**, 609–611.

Yeats, T.H., Buda, G.J., Wang, Z., Chehanovky, N., Moyle, L.C., Jetter, R., Schaffer, A.A. *et al.* (2012b) The fruit cuticle of wild tomato species exhibit architectural and chemical diversity, providing a new model for studying the evolution of cuticle function. *Plant J.* **69**, 655e666.

Supporting information

Additional supporting information may be found online in the Supporting Information section at the end of the article.

Figure S1 Expression by quantitative real-time PCR (qRT-PCR) of four *MADS* genes in the receptacle of *FaMADS9*-silenced lines at white and red stages.

Figure S2 Changes in primary metabolism in the receptacle of *FaMADS9*-silenced lines at three ripening stages.

Figure S3 Gene expression of genes involved in waxes and cutin biosynthesis.

Table S1 RNAseq full table.

Table S2 Differentially expressed genes in receptacle of WT and *FaMADS9*-silenced lines (L6 and L7) at white and red stage by RNAseq.

Table S3 Expression analysis of *Fragaria MADS* genes by RNAseq in receptacle of WT and *FaMADS9*-silenced lines (L6 and L7) at white and red stage.

Table S4 List of enriched genes from Mapman categories from Figure 2.

Table S5 Expression analysis of *Fragaria auxin-related* genes by RNAseq in receptacle of WT and *FaMADS9*-silenced lines (L6 and L7) at white and red stage.

Table S6 Expression analysis of *Fragaria NIP*, *PIP*, *TIP*, and *SIP* genes by RNAseq in receptacle of WT and *FaMADS9*-silenced lines (L6 and L7) at white and red stage.

Table S7 Relative metabolite content in fruits of FaMADS9-silenced plants.

Table S8 Expression analysis of *Fragaria ß-amylases*, *and Isoamylases* genes by RNAseq in receptacle of WT and *FaMADS9*-silenced lines (L6 and L7) at white and red stage.

Table S9 Expression analysis of *Fragaria L-ascorbic acid biosynthesis* genes by RNAseq in receptacle of WT and *FaMADS9*-silenced lines (L6 and L7) at white stage.

Table S10 Expression analysis of *Fragaria cell wall-modifying* genes by RNAseq in receptacle of WT and *FaMADS9*-silenced lines (L6 and L7) at white and red stage.

Table S11 Expression analysis of *Fragaria wax metabolism-related* genes by RNAseq in receptacle of WT and *FaMADS9*-silenced lines (L6 and L7) at white and red stage.

Table S12 ABA content of WT and *FaMADS9*-silenced red fruits.

Table S13 Tentatively identified metabolites in the UPLC-FT-ICR-MS and their abundancy in fruits of FaMADS9-silenced plants.

Table S14 Expression analysis of *Fragaria coumarate-coenzyme A ligase* (CL) genes by RNAseq in receptacle of WT and *FaMADS9*-silenced lines (L6 and L7) at white and red stages.

Table S15 List of dynamic gene interactions.

Table S16 GO analysis of the FaMADS9 targets from Table S15.

Table S17 Analysis of the 1 Kb promoter of *F. vesca* genes corresponding to putative FaMADS9 targets inferred from the GRN (Table S15).

Table S18 List of primers.